

Numerical investigations of various aspects of plaque deposition through constricted artery

P. Goswami^{1*}, D. K. Mandal², N. K. Manna¹ and S. Chakrabarti³

¹Department of Mechanical Engineering, Jadavpur University, Kolkata-700036, India

²Department of Mechanical Engineering, College of Engineering and Management,
Kolaghat-721171, West Bengal, India

³Department of Mechanical Engineering, Indian Institute of Engineering Science and
Technology, Shibpur, Howrah-711103, West Bengal, India

*Email: gospartha@gmail.com

ABSTRACT

The pulsatile blood flow through constricted artery generates fluid mechanical forces on internal layer of artery, endothelium. These fluid mechanical factors affect endothelial lining from keeping artery healthy. In this paper, a series of numerical simulations of modelled bell shaped stenosed artery have been carried out for investigation of fluid mechanical factors of realistic pulsatile flow at the inlet of modelled stenosis with bell shaped geometry. The governing equations for two-dimensional unsteady laminar flow of incompressible fluid are solved by finite volume method followed by SIMPLER algorithm. The fluid mechanical factors, particularly wall pressure, streamline contour, peak wall shear stress, low wall shear stress and oscillatory shear index, having inferences to the arterial disease, are investigated by simulation results of different percentage of restrictions. The impacts of Reynolds number and Womersley number for both of mild stenosis and severe stenosis on arterial disease, atherosclerosis are also investigated by evaluating fractional flow reverse and oscillatory shear potential. All these parameters have a noticeable impact for the plaque deposition. The possibility of plaque deposition at the downstream of the stenosis in a stenosed artery always increases with increase in Reynolds number of flow, percentage of restriction and Womersley number of flow.

Keywords: Wall pressure; wall shear stress; fractional flow reverse; oscillatory shear potential; atherosclerosis

INTRODUCTION

Constricted artery is a mimic of stenosed artery. Stenosis, a narrowing in lumen area of an artery, is caused by the arterial disease, atherosclerosis. Now days, atherosclerosis, a big problem in human life, is processed by deposition of plaque at inner lining i.e. endothelium of an artery wall. Plaque is buildup of cholesterol, fatty substances, cellular waste products, calcium and fibrin etc. The plaque may block partially or totally the lumen area of artery and then it initiates the cardiovascular diseases such as gangrene, thrombus, heart attack etc. High level of cholesterol and triglycerides in blood, cigarette smoking and high blood pressure are

taken into account for progression of atherosclerosis by many researchers. Generally the symptoms of atherosclerosis are exposed in advanced stages and then instant surgical intervention is only way to tackle the patient situation. The main challenge is now to detect the plaque deposition at very early stage and to predict the severity of plaque development for surgical intervention. The flow characteristics of blood flow through artery play an important role for initiation, progression and development of plaque inside artery wall. The pulsatile nature of blood flow generates fluid mechanical forces acting on the internal layer of artery, endothelium. The endothelium creates biochemical signal to keep artery wall healthy under different physiological conditions. Blood pressure exerts force, which is directed in the perpendicular direction of artery wall. Thus the artery wall having circular cross-section will be stretched circumferentially and creates circumferential stress. The circumferential stress is associated with the tearing of endothelium layer of artery as well as plaque rupture and as a result, possibility of plaque deposition inside artery wall increases. Plaques deposit in the regions of low pressure because a suction action exerted on the surface endothelium eventually causes the layer to be selectively separated from adjacent tissue. This tearing action is thought to cause damage, in turn, to the endothelium and adjacent wall layers, with subsequent thickening of the intima and eventual plaque development [1]. The pulsatile blood flow creates fluctuating tangential forces acting over the internal layer of artery (wall shear stress). The fluctuation of wall shear stress inflames the biochemical signal to initiate the plaque deposition. The high shear stress harms the artery wall mechanically and thereby promotes the diseases, atherosclerosis [2]. These high levels of wall shear stress also cause direct endothelial damage by platelets activation and increase the risk of clotting the blood flow [3]. This condition is very probable in atherosclerosis disease and basically the main cause of heart attacks [4]. This high shear stress activates platelets and thus induces thrombosis, a cardio vascular disease. Thrombosis fully restricts blood flow to the heart or brain through artery [5]. Low shear stress in the separation region is considered to be related to the mass transportation across the arterial wall and long “dwell time” for platelet endothelium interaction [6]. These regions with low shear stress and flow recirculation are susceptible to fatty deposition [7]. At present, a lot of scientific researchers are engaged to add more and more information in this field. Rikhtegar et al. [8] have investigated wall shear stress, oscillatory shear index (OSI), relative residence time (RRT) for the prediction of plaque development. Bit and Chattopadhyay [9] have investigated OSI, WSS for different degree of stenosis of hemodynamic flow through stenosed artery considering realistic pulsatile flow at inlet. Peng et al. [10] have demonstrated the impact of stenosis geometry on the wall shear stress, recirculation zone and the fractional flow reverse for flow through stenotic coronary artery. Wall shear stress and oscillatory shear index distribution have been studied by Basasvaraja et al. [11] for flow through carotid artery for varying degree of stenosis. Liu et al. [12] have investigated pulsatile flow through stenosed tapered artery using finite difference method on non-uniform grid. Lee et al. [13] have studied sinusoidal fluctuated pulsatile laminar flow through various constrictions by finite volume method using non-staggered non-orthogonal grid.

In the present research work, it is contemplated on the various aspects of plaque deposition in connection to the fluid mechanical factors, which have not been met clearly in the previous studies. An attempt has been made to investigate, fluid mechanical factors such as, wall pressure, wall shear stress, oscillatory shear index, fractional flow reverse and oscillatory shear potential, which have strong impact for plaque deposition, for realistic

pulsatile flow through bell shaped stenosed artery. In this work, the numerical solutions are obtained under the conditions of homogeneous, incompressible and Newtonian fluid through axially symmetric rigid stenosis. The blood flow has been considered as two-dimensional, laminar and pulsatile flow. It has been known that the blood usually behaves as a non-Newtonian fluid. But, in large arteries, especially at moderate to high shear rates [5, 14 and 15] i.e. less than 1 s^{-1} , blood may be regarded as a Newtonian fluid. The assumption of rigid boundary does not seriously affect the results in most cases, since the development of atherosclerosis in arteries causes a considerable reduction in the elastic property of its wall [16].

NUMERICAL MODELING

Schematic diagram of the computational domain of artery model with bell shaped stenosis is illustrated in Figure 1. This bell-shaped stenosis [17] geometry is modelled mathematically as the following equation.

$$r = 0.5 - h_f \exp\left(-\frac{4m^2 z^2}{L_s^2}\right) \quad (1)$$

Where, m is a parametric constant, which defines shape of stenosis. In medical practice, percentage stenosis or percentage of restriction is commonly defined as percentage occlusion by diameter [18]. Dimensions of stenosis model for different percentage of restrictions are given in Table 1.

$$PR = \frac{D - (D/2 - h_f)}{D} \times 100\% \quad (2)$$

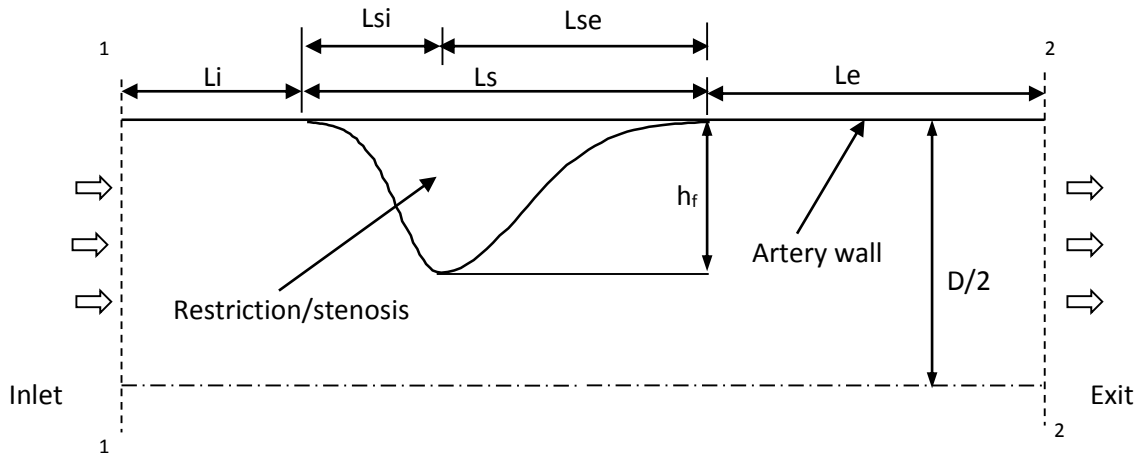


Figure 1. Computational domain of artery model

Table 1: Dimensions of Stenosis Models with Different Percentage of Restrictions

Dimensions	h _f	D	L	L _i	L _s	L _{si}	L _{se}
PR 30%	0.15	1	200	49.9	0.2	0.1	0.1
PR 50%	0.25	1	200	49.9	0.3	0.1	0.2
PR 70%	0.35	1	200	49.9	0.4	0.1	0.3

For this axisymmetric flow of incompressible and Newtonian fluids with constant fluid properties, the governing equations are the continuity and Navier-Stokes equations in two-dimensional cylindrical co-ordinates (r,z). The governing equations are non-dimensionalized with the following dimensionless variables.

Lengths: $r^* = r/D, z^* = z/D, L^* = L/D, t^* = t/T$. Velocities: $u_r^* = u_r/U, u_z^* = u_z/U$ and Pressure: $p^* = p/\rho U^2$.

The non-dimensional governing equations, Equations (3-5), are:

$$\frac{1}{r^*} \frac{\partial(r^* u_r^*)}{\partial r^*} + \frac{\partial u_z^*}{\partial z^*} = 0 \tag{3}$$

$$\frac{1}{\pi} \frac{W_o^2}{Re} \frac{\partial u_r^*}{\partial t^*} + u_r^* \frac{\partial u_r^*}{\partial r^*} + u_z^* \frac{\partial u_r^*}{\partial z^*} = -\frac{\partial p^*}{\partial r^*} + \frac{2}{Re} \left[\frac{\partial^2 u_r^*}{\partial r^{*2}} + \frac{\partial^2 u_r^*}{\partial z^{*2}} + \frac{1}{r^*} \frac{\partial u_r^*}{\partial r^*} \right] \tag{4}$$

$$\frac{1}{\pi} \frac{W_o^2}{Re} \frac{\partial u_z^*}{\partial t^*} + u_r^* \frac{\partial u_z^*}{\partial r^*} + u_z^* \frac{\partial u_z^*}{\partial z^*} = -\frac{\partial p^*}{\partial z^*} + \frac{2}{Re} \left[\frac{\partial^2 u_z^*}{\partial r^{*2}} + \frac{\partial^2 u_z^*}{\partial z^{*2}} + \frac{1}{r^*} \frac{\partial u_z^*}{\partial r^*} - \frac{u_z^*}{r^{*2}} \right] \tag{5}$$

Where W_o is the Womersley number, which is defined by equation (6) and Re is the Reynolds number, which is defined by following equation.

$$W_o = R \sqrt{\frac{\omega}{\nu}} \tag{6}$$

Where ω is the radial frequency $2\pi/T$. The Womersley number can be interpreted as the ratio of unsteady force to viscous force. The Womersley number is an indicator of the main frequency of the pulsatile flow. In this work, two different values of Womersley number are taken as 5 and 12.5 from different physiological conditions of the body. In this work, the Reynolds number is considered as 50 and 200.

At this problem, four different types of boundary conditions are applied to solve the governing equations. No slip condition at the artery wall is applied, i.e., $u_r^* = 0, u_z^* = 0$.

At the inlet, axial velocity has been specified as realistic pulsatile flow condition, as can be seen in Figure 2 and Equation (7) [19], and the transverse velocity has been set to zero, i.e.,

$$u_z^* = 1 + 0.29244 \cos(\omega t^* + 4.027) - 0.5908 \cos(2\omega t^* + 6.509) + 0.2726 \cos(3\omega t^* + 1.913) + 0.1980 \cos(4\omega t^* + 1.461) + 0.1124 \cos(5\omega t^* + 0.074) \tag{7}$$

$u_r^* = 0$. At the exit, fully developed flow condition has been assumed and hence gradients have been set to zero, i.e., $\partial u_z^* / \partial z^* = 0, \partial u_r^* / \partial z^* = 0$. The normal gradient of the axial velocity and the transverse velocity have been set to zero at the line of symmetry, i.e., $\partial u_z^* / \partial r^* = 0, u_r^* = 0$. The boundary conditions are shown in Figure 1a.

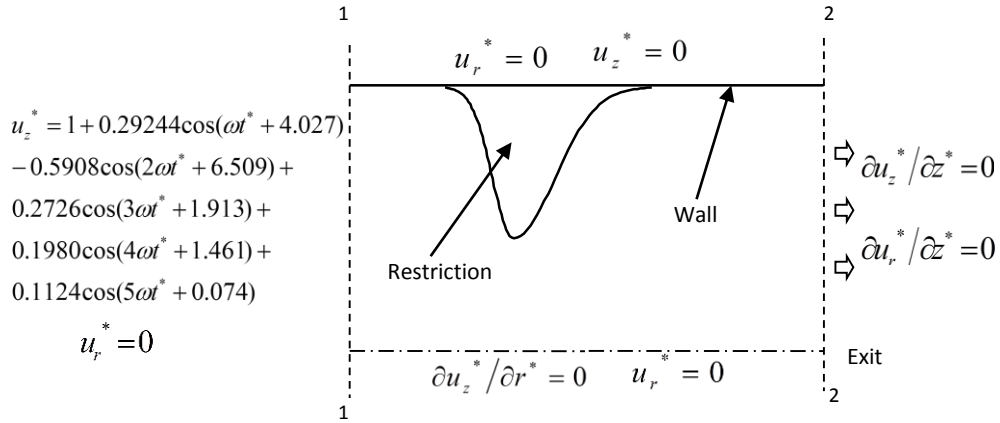


Figure 1a. Schematic diagram of modeled artery with boundary conditions

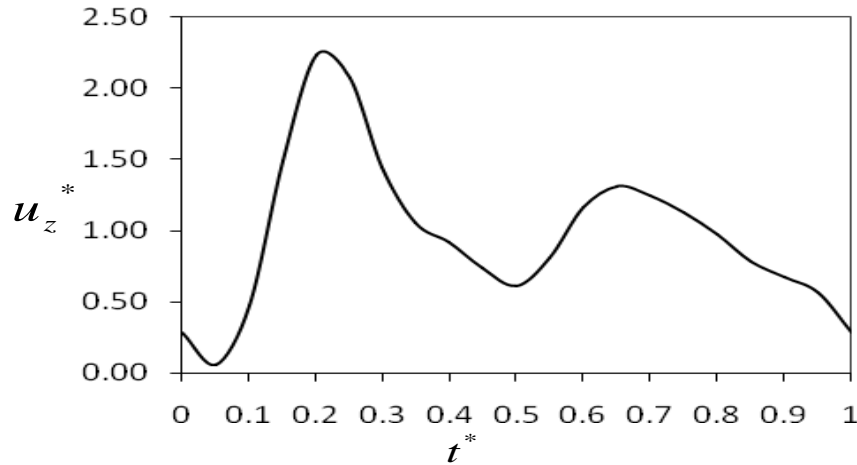


Figure 2. Axial velocity distribution

In this present study, the governing equations have been solved numerically by an in-house CFD code developed using integral approach of the finite volume method. The governing equations are discretized by control volume formulation on a staggered grid. Non-uniform mesh type is used in this finite volume method. Finer grid near wall and restriction, and coarser grid for other parts of pipe are taken for fast and more accurate results. The equations are integrated over proper control volume and the values of pressure are stored at centre of control volume and values of both velocities are stored at faces of control volume. The discretized equations are solved using Tri-diagonal Matrix Algorithm (TDMA) with Alternate Direction Implicit (ADI) scheme following Semi-Implicit method for Pressure-Linked Equations Revised (SIMPLER) algorithm [20]. The third-order upwind scheme has been used line by line for discretization of advective equations. The discretized equations have been solved. The convergence of the iterative scheme has been achieved when the normalized residuals for mass and momentum equations summed over the entire calculation domain will fall below 10^{-7} . In the computation, the non-dimensional length of computational domain has been chosen to be 200. After grid independence test, finally the numerical mesh comprised of 449×49 (22001 node numbers) grid nodes in z and r direction has been considered in the present work.

RESULTS AND DISCUSSION

The numerical results obtained from the simulation using the in-house CFD code are compared with the numerical and experimental results of Womersley [21] and Ojha et al. [22] respectively. The differences between the predictions and experimental data are found to be a good agreement, which is shown by our previous published work, Goswami et al. [23]. Time-averaged wall pressure, fractional flow separation, peak time-averaged wall shear stress, low time-averaged wall shear stress, oscillatory shear index and endothelial cell activation potential have been taken into consideration for the analyzing of fluid mechanical features of realistic pulsatile flow through the stenosed arteries with mild stenosis (PR 30%), moderate stenosis (PR 50%) and severe stenosis (PR 70%).

The time-averaged wall pressure is calculated by integrating instantaneous wall pressure over a cardiac cycle. The variation of the time-averaged wall pressure along the axial direction of the considered arterial length is shown in Figure 3 for all considered percentage of restrictions with fixed Re 100 and Wo 10. The wall pressure at the outlet of the modeled artery has been set to zero for all considered cases. The wall pressure decreases gradually from inlet to outlet of the artery with a pressure drop at the throat of the stenosis for each percentage of restriction. From the figure, it is also noted that the wall pressure before stenosis and wall pressure drop are higher for higher percentage of restriction. Thus higher percentage of restriction is more prone to plaque rupture as well as tearing of endothelium layer, which in turn allows plaques to form. The axial distribution of time-averaged wall pressure for mild stenosis and severe stenosis is shown in Figure 4 and Figure 5 respectively. From the figures, it is noticed that the wall pressure before stenosis and pressure drop at the stenosis decrease with increase in Reynolds number for both of mild and severe stenosis. As the wall pressure is non-dimensionalized by dividing it with averaged velocity in the mathematical formulation, it may commented that the wall pressure before stenosis and pressure drop at the stenosis increase with increase in Reynolds number for both of mild and severe stenosis. As a result, possibility of plaque deposition is higher for higher value of Reynolds number. Viewing on the figures, it can also be mentioned that wall pressure before stenosis decrease prominently with increase in Womersley number for both of mild and severe stenosis. So plaque deposition chance is high for lower value of Womersley number. Further, it can be also pointed out that the effect of Womersley number on wall pressure drop is not so evidenced, but the wall pressure drop increases with increase in Womersley number. As a result, plaque deposition chance increases by increase in Womersley number for both of mild and severe stenosis.

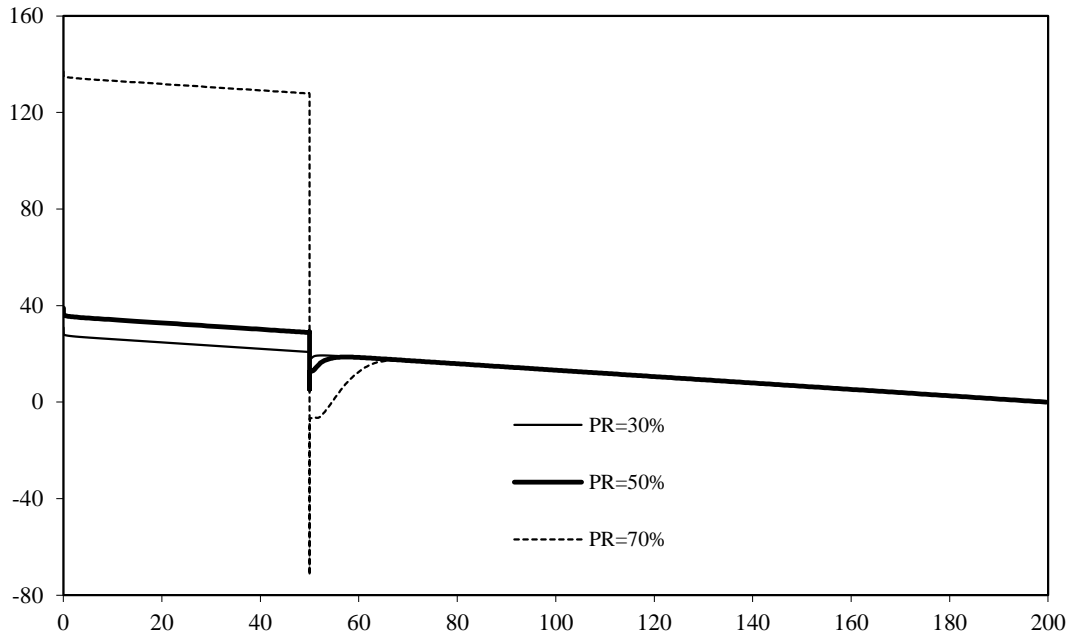


Figure 3. Distribution of wall pressure along axial direction for fixed Re 100 and Wo 10 for different PR

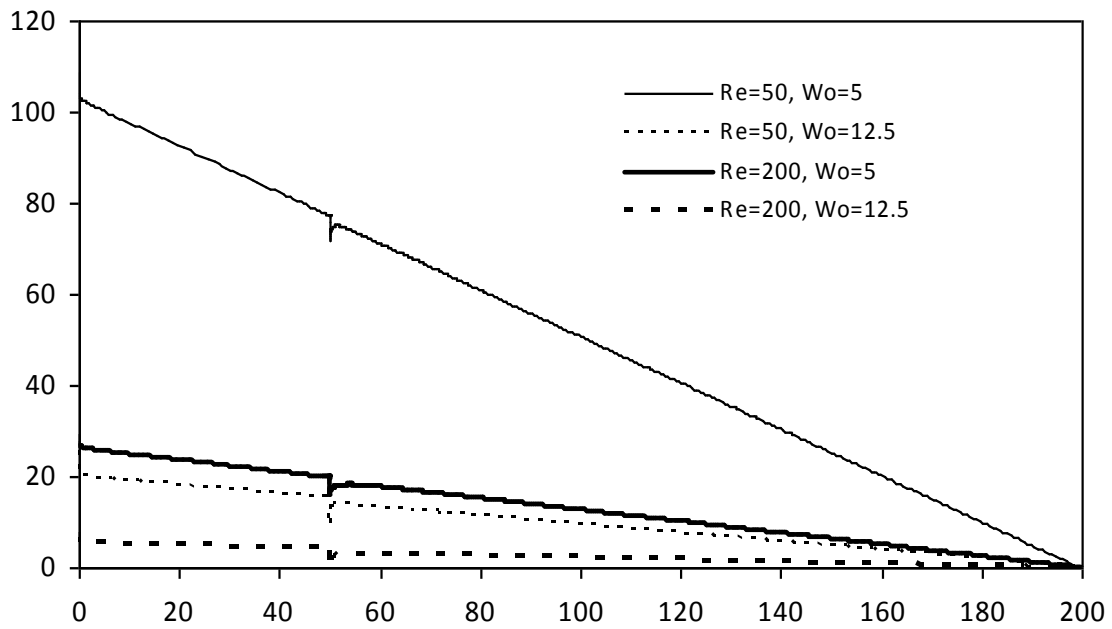


Figure 4. Distribution of wall pressure along axial direction for PR 30% with different Re and different Wo

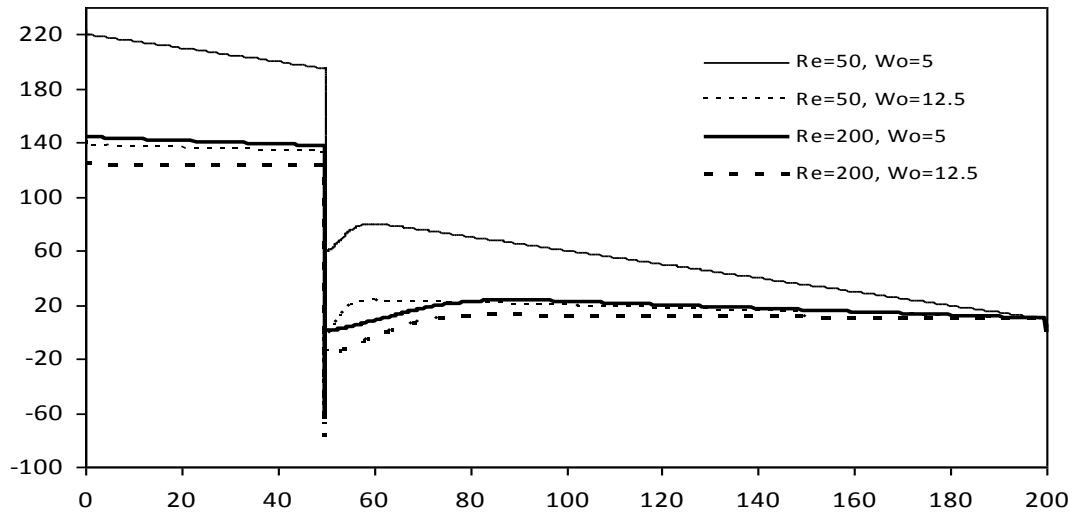


Figure 5. Distribution of wall pressure along axial direction for PR 70% with different Re and different Wo

Recently, fractional flow reserve (FFR) is incorporated in clinical practice for diagnostic categorization and medical recommendation [24, 25]. Higher value of FFR indicates severity of arterial stenosis in certain circumstances. FFR is the ratio of pressure at distal to stenosis and pressure at proximal to stenosis. FFR has been estimated from the simulation results for different combination cases of percentage of restriction, Reynolds number and Womersley number. From the Figure 6, it is noted that FFR value is always greater than 8.0 for severe stenosis (PR 70%) and less than 4.5 for mild stenosis (PR 30%). As the wall pressure is non-dimensionalized with averaged velocity, it can be commented that FFR increases with increase in Reynolds number for both of mild and severe stenosis. Though the effect of Womersley number on FFR is not so significant for severe stenosis but it is prominent for mild stenosis. FFR value decreases with increase in Womersley number for the case of mild stenosis. From overall study on FFR, it is mentioned that higher FFR indicates higher percentage of restriction of flow with high Reynolds number and low Womersley number. So Reynolds number and Womersley number of pulsatile flow are to be considered before surgical intervention.

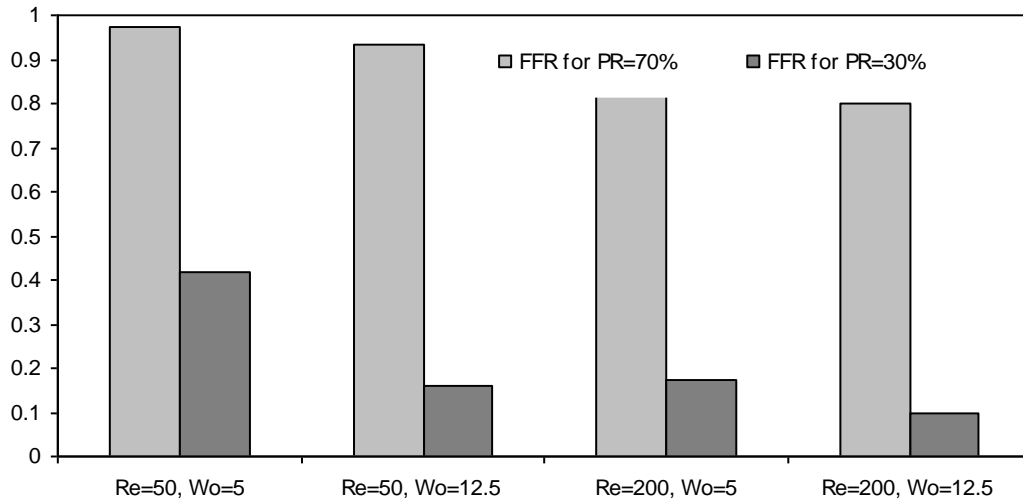


Figure 6. Fractional flow reverse for different combination cases of percentage of restriction, Reynolds number and Womersley number

The details of flow fields are also investigated for three different percentage of restrictions at four different times of a cardiac cycle such as $t/T=0$, $t/T=0.25$, $t/T=0.50$ and $t/T=0.75$. By assessing all the instantaneous streamline patterns at different time steps for different percentage of restrictions, as can be seen in Figure 7a-7d, it is obvious that higher percentage of restriction leads to higher flow separation with stronger formed vortex in the downstream of stenosis. Therefore, it may be commented that chances of development of atherosclerotic plaque at the inner wall of artery increase with increase in percentage of restriction.

As blood flow velocity changes in the constricted region, it is very important to notice the wall shear distribution in the stenotic zone. The time-averaged wall shear stress is calculated by integrating instantaneous wall shear stress, obtained from the simulation results at different time levels, over a cardiac cycle. The variation of the time-averaged wall shear stress along axial direction in the stenotic zone for different percentage of restriction is shown in Figure 8. It is revealed that the nature of variation of peak WSS is almost similar for all the considered percentage of restriction. Peak wall shear stress increases sharply proximal to the throat of the stenosis and time-averaged wall shear stress decreases sharply distal to the throat. From the figure, it is observed that the magnitude of peak wall shear stress increases with increasing in percentage of restriction. So the possibility of plaque deposition is high for higher percentage of restriction. Figure.9 depicts the variation of wall shear stress along axial direction at the post-stenotic zone for various percentage of restriction. From the figure of low wall shear stress, it is observed that the low wall shear stress enhances with increase in percentage of restriction. Zero magnitude of time-averaged wall shear stress indicates the location of stagnation points as well as separation and reattachment points. The increment of low

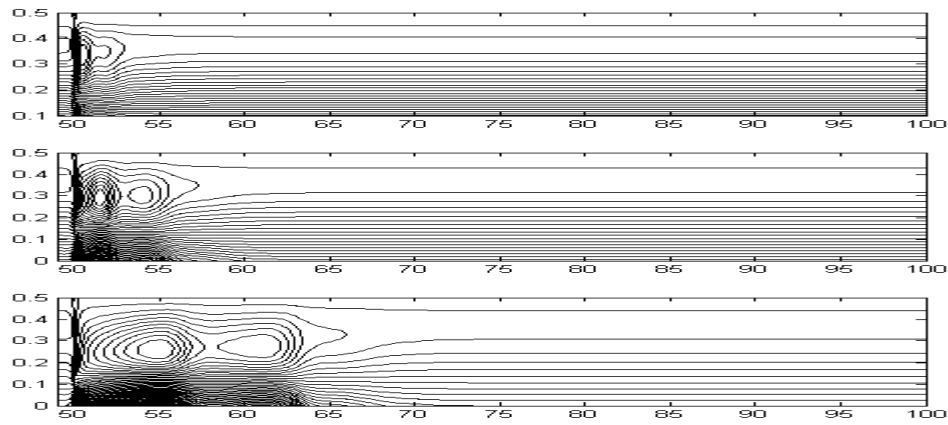


Figure 7a. Streamline contour for PR 30%, PR 50% and PR 70% (top to bottom) respectively at $t^*=0$

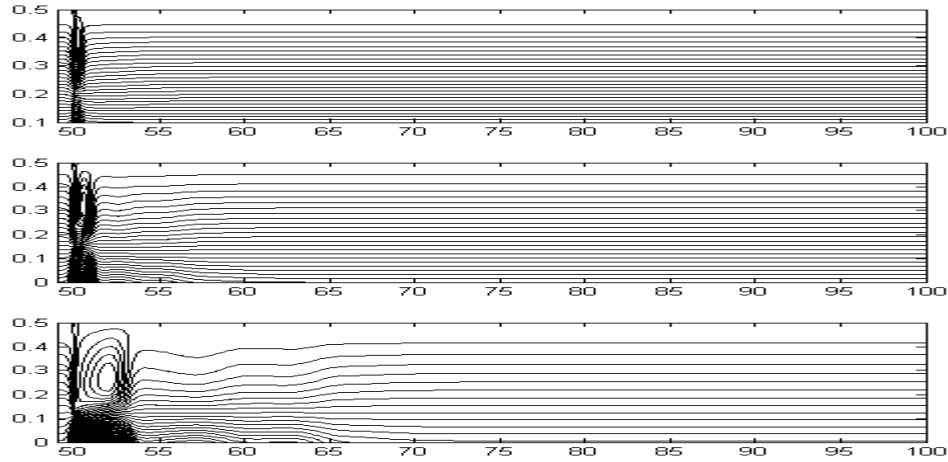


Figure 7b. Streamline contour for PR 30%, PR 50% and PR 70% (top to bottom) respectively at $t^*=0.25$

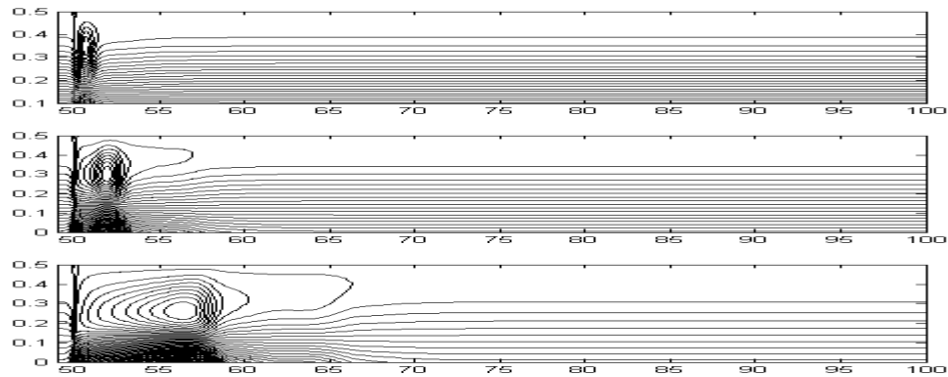


Figure 7c. Streamline contour for PR 30%, PR 50% and PR 70% (top to bottom) respectively at $t^*=0.5$

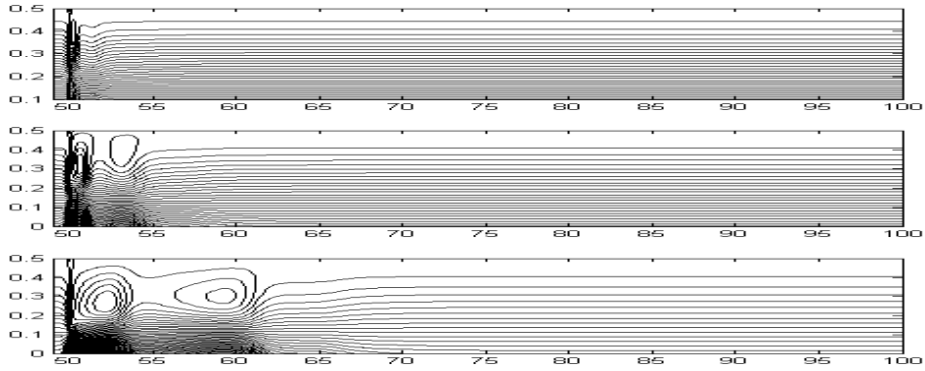


Figure 7d. Streamline contour for PR 30%, PR 50% and PR 70% (top to bottom) respectively at $t^*=0.75$

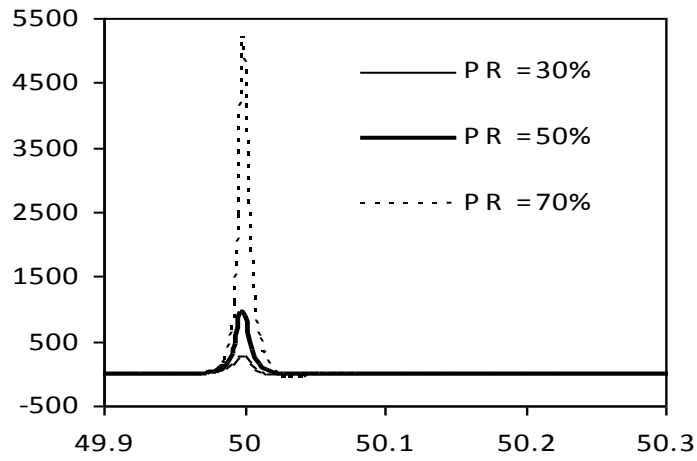


Figure 8. Distribution of peak WSS for Re 100 and Wo10

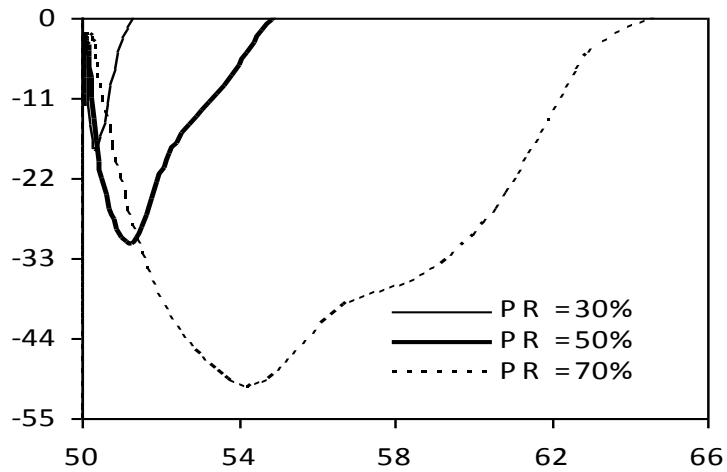


Figure 9. Distribution of low WSS for Re 100 and Wo10

wall shear stresses with higher percentage of restriction and the corresponding formation of separating region may damage the endothelial layer of artery.

The fluctuation in wall shear stress is measured by oscillatory shear index. Oscillatory Shear Index (OSI) is a derivative of wall shear stress. OSI defines the cyclic departure of the WSS vector from its major axial direction [26, 27]. The OSI is calculated from the following formula (Equation (8)):

$$OSI = \frac{1}{2} \left[1 - \frac{\left| \int_0^T \tau_w dt \right|}{\int_0^T |\tau_w| dt} \right] \quad (8)$$

The distribution pattern of the OSI along axial direction of arterial length in the stenotic zone and post stenotic zone is shown in Figure 10 for three different percentages of restrictions. The figure clearly indicates that the first peak OSI just immediate after throat of the stenosis and the location of time-averaged reattachment point i.e. second peak OSI at the downstream of stenosis are greatly influenced by percentage of restriction. Increase or decrease of first peak OSI does not obey any proportionality rule with percentage of restriction, but higher percentage of restriction always leads to longer recirculation length for all combination case and subsequently increases the chance of formation of atherosclerosis. So the chance of plaque deposition at the inner wall of artery

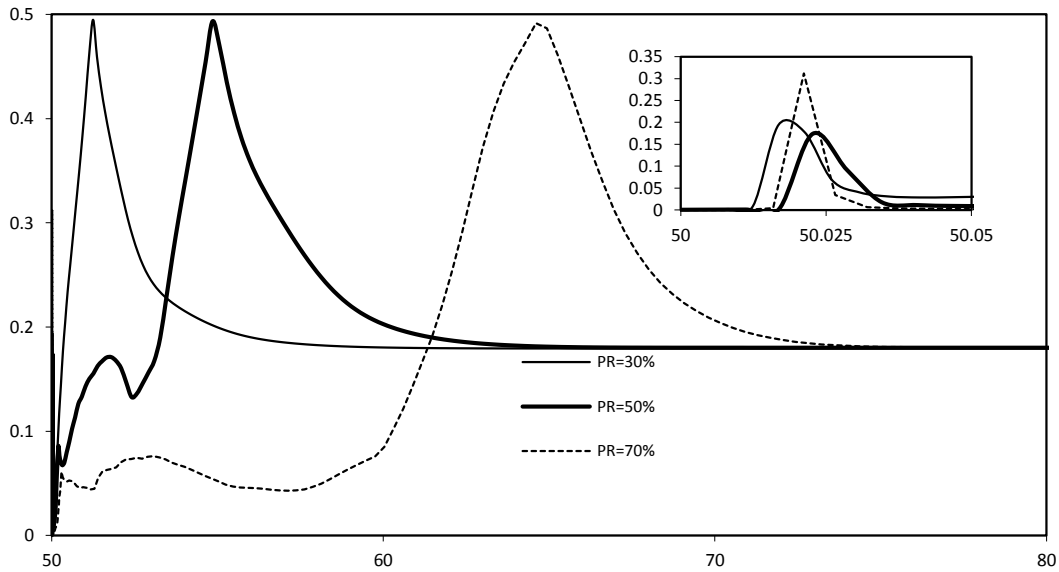


Figure 10. Distribution of oscillatory shear index along axial direction for Re 100 and Wo 10

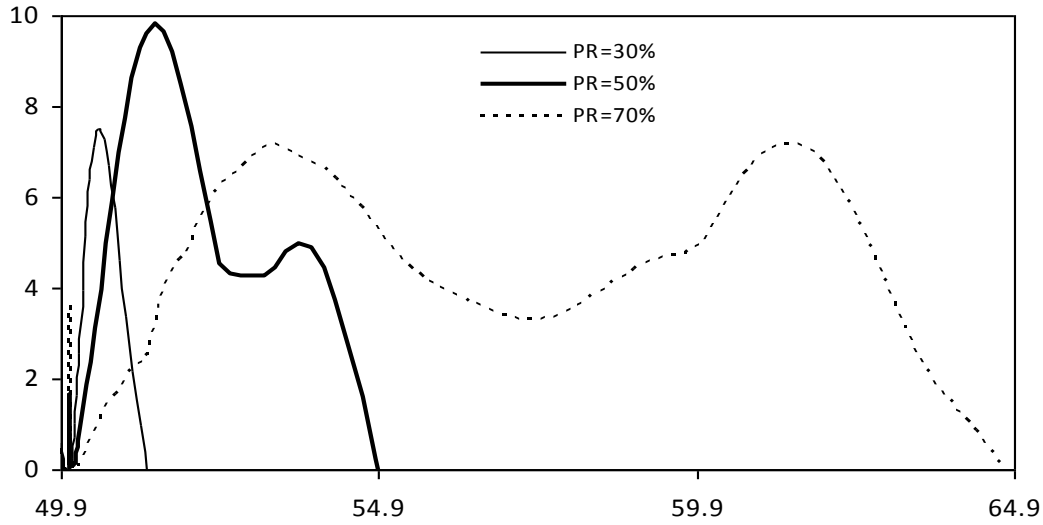


Figure 11. Distribution oscillatory shear potential of along axial direction for fixed Re 100 and Wo 10

due to existence of recirculation zone increases with increase in percentage of restriction. This low averaged shear stress and high OSI may be significant condition in the development and localization of atherosclerotic plaque in the inner wall of artery as suggested by Ku et al. [26]. Endothelial cell activation potential (ECAP) was proposed by Achille et al.[28] to localize regions of wall exposed to both high OSI and low WSS using the ratio of these two indices for blood flow through aneurysm. In the study of blood flow through stenosed artery, both high OSI always having positive value and low WSS having negative value localize in post-stenotic zone, as can be seen in Figure 9 and Figure 10. To combine high OSI and low WSS, a single parameter, named as oscillatory shear potential (OSP) is proposed for case of blood flow through stenosed artery. The OSP is calculated with the following formulae, Equation(9):

$$OSP = -2 \times OSI \times \overline{\tau_w^*} \quad (9)$$

Higher value of OSP at any location of artery wall implies that the wall is under low wall shear stress as well as high OSI. Figure.11 illustrates the distribution of OSP along axial direction for different percentage of restriction. The figure clearly depicts that OSP moves towards downstream of stenosis further as percentage of restriction increases. The higher percentage of restriction leads to larger area under OSP. As a result, the chance of plaque deposition increases with increase in percentage of restriction. The effect of Reynolds number and Womersley number for both the mild stenosis and severe stenosis on OSP is depicted in Figure 12 and Figure 13 respectively. From the figure, it is noticed that area under OSP increases with increase in Reynolds number as well as Womersley number of flow for both mild and severe stenosis. OSP also move towards downstream of stenosis as Reynolds number increases. Therefore, it is mentioned that the possibility of plaque deposition inside the artery wall always increases with increase in Reynolds number and Womersley number for any percentage of restriction.

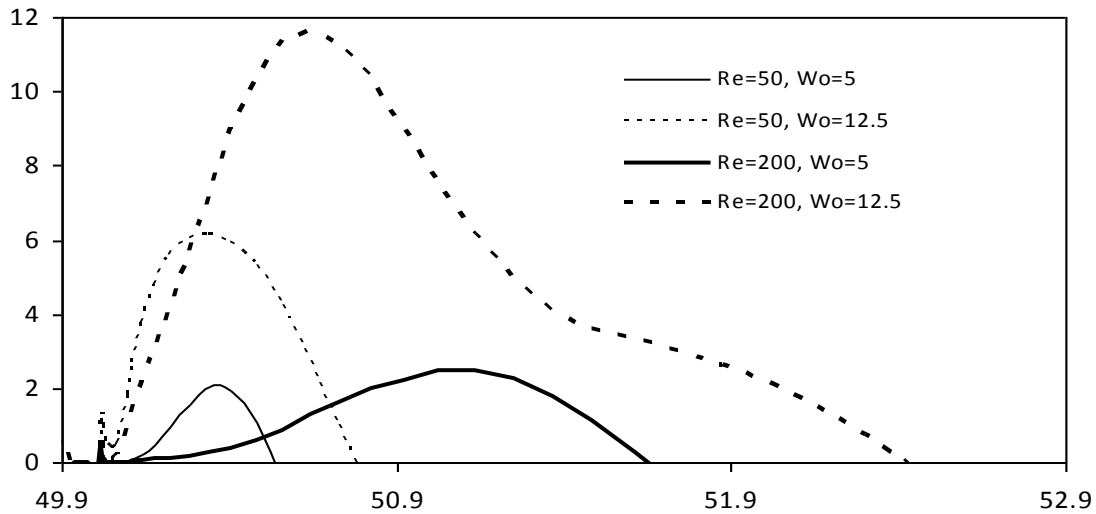


Figure 12. Distribution of oscillatory shear potential along axial direction for PR 30%

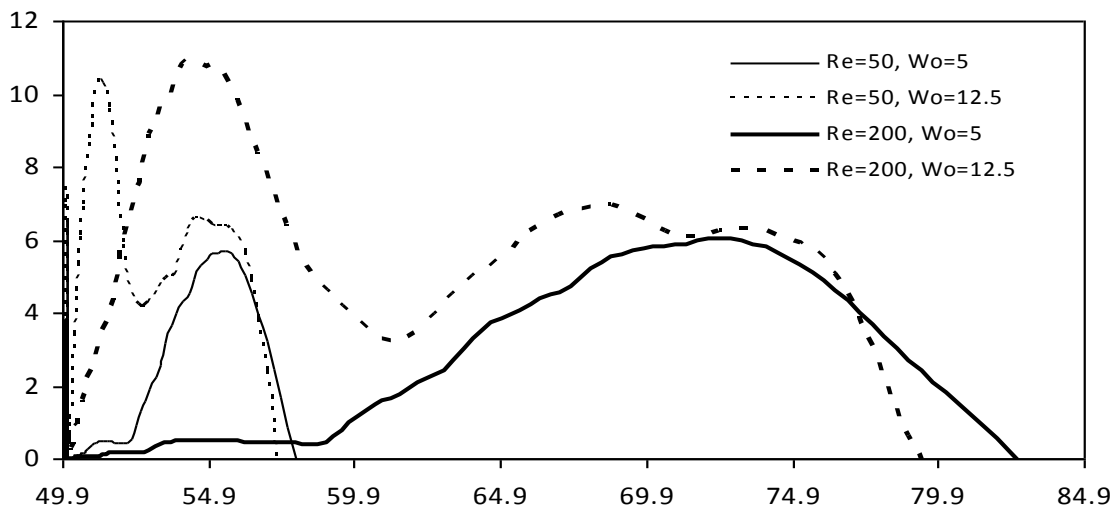


Figure 13. Distribution of oscillatory shear potential along axial direction for PR 70%

CONCLUSIONS

The aim of this present work is to investigate fluid mechanical factors having inferences to plaque deposition in a realistic pulsatile flow through bell-shaped stenosed artery for different percentage of restrictions, Reynolds numbers of flow and Womersley numbers of flow.

Wall pressure before stenosis and wall pressure drop at stenosis increase with increase in percentage of restriction and Reynolds number of flow, but decreases with increase in Womersley number of flow. FFR value is higher for higher percentage of restriction. To detect percentage of restriction with FFR value, Reynolds number and Womersley number flow should be taken into consideration.

Both peak and low wall shear stress increase with increase in percentage of restriction. The first and second peaks OSI are found at stenotic zone and post-stenotic zone respectively. The recirculation zone is identified in the downstream of stenosis and the size of the recirculation zone increases with increase in percentage of restriction.

Oscillatory shear potential combines oscillation in wall shear stress and low wall shear stress. The area under OSP increases with increase in percentage of restriction, Reynolds number and Womersley number for both mild and severe stenoses.

The possibility of plaque deposition at the downstream of the stenosis in a stenosed artery always increases with increase in Reynolds number of flow, percentage of restriction and Womersley number of flow.

In conclusion, the present study has pointed out that the fluid mechanical factors, mainly fractional flow reverse and oscillatory shear potential, may be useful to predict the risk of the plaque deposition in constricted artery and may help to decide on the proper medical management for the patient having stenosis.

NOMENCLATURE

D	Diameter of the artery	T	Time period of the pulsatile cycle
R	Radius of artery	t	Time
L	Total length of computational domain	p	Static pressure
L_i	Length of computational domain before stenosis	Re	Reynolds Number = $\frac{\rho UD}{\mu}$
L_s	Length of stenosis	Wo	Womersley number = $\frac{D}{2} \sqrt{\frac{2\pi}{\nu T}}$
L_{si}	Length of upstream stenosis	p_w	Wall pressure
L_{se}	Length of downstream stenosis	τ_w	Wall shear stress (WSS), [Nm ⁻²]
L_e	Length of computational domain after stenosis	OSP	Oscillatory shear potential
h_f	Height of stenosis	WSS	Wall shear stress
u_z	Velocity in z-direction	FFR	Fractional flow reverse
u_r	Velocity in r-direction	OSI	Oscillatory shear index
U	Average velocity in r-direction at inlet	$\overline{\tau_w^*}$	Time-averaged wall shear stress
μ	Dynamic viscosity	PR	Percentage of restriction
ρ	Density	1-1	Inlet
ν	Kinematic viscosity	2-2	Exit
Superscripts		r, z	Cylindrical co-ordinates
*	Dimensionless terms		

REFERENCES

- [1] Gessner FB. Haemodynamic theories of atherogenesis, *Circulation Research*. September 1973; 3:259-266.
- [2] Fry DL. Acute vascular endothelial changes associated with increased blood velocity gradients. *Circulation Research*. 1968; 12:165-97.
- [3] Malek AM, Alper SL and Izumo S. Hemodynamic shear stress and its role in atherosclerosis. *JAMA*. 1999; 282, 2035-2042.
- [4] Razavi A, Shirani E and Sadeghi MR. Numerical simulation of blood pulsatile flow in a stenosed carotid artery using different rheological models. *Journal of Biomechanics*. 2011; 44:2021–2030.
- [5] Ku DN. Blood flow in arteries. *Annual Review of Fluid Mechanics*. 1997; 29:399-434.
- [6] Caro CG, F-G JM and Schroter RC. Atheroma and arterial wall shear: observation, correlation, and proposal for a shear dependent mass transfer mechanism for atherogenesis. *Proceedings of the Royal Society of London. Series B, Biological Sciences*. 1971; 117:109-159.
- [7] Caro CG. Discovery of the role of wall shear in atherosclerosis. *Arteriosclerosis, Thrombosis and Vascular Biology*. 2009; 29, 158-162.
- [8] Rikhtegar F, Knight JA, Olgac U, Saur SC, Poulidakos D, Marshall W, Cattin PC, Alkadhi H, Kurtcuoglu V. Choosing the optimal wall shear parameter for the prediction of plaque location a patient-specific computational study in human left coronary arteries. *Atherosclerosis*. 2012; 221(2):432–7.
- [9] Bit A and Chattopadhyay H. Numerical investigations of pulsatile flow in stenosed artery. *Acta of Bioengineering and Biomechanics*. 2014; 16(4):33-44.
- [10] Peng C, Wang X, Xian Z, Liu X, Huang W, Xu P, and Wang, J. The impact of the geometric characteristics on the hemodynamics in the stenotic coronary artery. *PLoS One*. 2016; 11(6): e0157490.
- [11] Basavaraja P, Surendran A, Gupta A, Saba L and Laird J R. Wall shear stress and oscillatory shear index distribution in carotid artery with varying degree of stenosis: A hemodynamic study. *Journal of Mechanics in Medicine and Biology*. 2017; 17(2):1750037.
- [12] Lee TS, Liu X, Li GC and Low HT. Numerical study on sinusoidal fluctuated pulsatile laminar flow through various constrictions. *Communication in Computational Physics*. 2007; 2(1):99-122.
- [13] Liu G, Tao W, Xian-J, Quan AB and Liu LG. Numerical study of pulsating flow through a tapered artery with stenosis. *Chinese Journal of Physics*. 2004; 42(4-I):401-409.
- [14] Pedley TJ. *The Fluid mechanics of large blood vessels*. Cambridge University Press. 1980.
- [15] Fung YC. *Biomechanics: Circulation*, 2nd edition. Springer. 1997.
- [16] Liu G, Tao W, Xian-J, Quan AB and Liu LG. Numerical study of pulsating flow through a tapered artery with stenosis. *Chinese Journal of Physics*. August 2004; 42, No.4-1:401-409.
- [17] Misra JC and Shit GC. Blood flow through arteries in a pathological state: a theoretical study. *International Journal of Engineering Science*. 2006; 44:662-671.

- [18] Wootton DM and Ku DN. Fluid mechanics of vascular systems, diseases, and thrombosis. *Annual Review of Biomedical Engineering*. 1999; 1:299–329.
- [19] Adib MAHM, Li S, Watanabe Y, Wada S. Minimizing the blood velocity differences between phase-contrast magnetic resonance imaging and computational fluid dynamics simulation in cerebral arteries and aneurysms. *Medical & Biological Engineering & Computing*. 2017;55,9:1605-1619.
- [20] Patankar SV. *Numerical heat transfer and fluid flow*, Hemisphere Publication. 1980.
- [21] Womersley JR. Method for the calculation of velocity, rate of flow, and viscous drag in arteries when the pressure gradient is known. *Journal of Physiology*. 1955; 127:553-563.
- [22] Ojha M, Cobbold C, Johnston KW and Hummel RL. Pulsatile flow through constricted tubes: an experimental investigation using photochromic tracer methods. *Journal of Fluid Mechanics*. 1989; 203:173-197.
- [23] Goswami P, Mandal DK, Manna NK and Chakrabarty S. Study on the effect of steady, simple pulsatile and physiological pulsatile flows through a stenosed artery. *Heat Mass Transfer*. 2014; 50, 1343-1352.
- [24] Kim J and Koo B. Fractional flow reserve: the past, present and future. *Korean Circulation Journal*. 2012; 42:441-446)
- [25] Pijls NHJ, Sels JW. Functional measurement of coronary stenosis. *Journal of the American college of cardiology*. 2012; 59(12):1045–1057.
- [26] Ku DN, Giddens DP, Zarins CK and Glagoy S. Pulsatile flow and atherosclerosis in the human carotid bifurcation—positive correlation between plaque location and low and oscillating shear– stress. *Arteriosclerosis*. 1985; 5:293-302.
- [27] He X and Ku DN. Pulsatile flow in the human left coronary artery bifurcation: average conditions. *Journal of Biomechanical Engineering*. 1996; 118: 74-82.
- [28] Di Achille P, Tellides G, Figueroa CA and Humphrey J D. A haemodynamic predictor of intraluminal thrombus formation in abdominal aortic aneurysms. *Proceedings of the Royal Society of London Mathematics Physics Engineering Sciences*. 2014; 470:20140163.